



HAL
open science

Enhanced conductivity and photoelectric performance of GeSe₂-Sb₂Se₃-based glass ceramics by CuI doping

Y. Xu, H. Jin, Y. Liu, B. Fan, H.-L. Ma, Xianghua Zhang

► To cite this version:

Y. Xu, H. Jin, Y. Liu, B. Fan, H.-L. Ma, et al.. Enhanced conductivity and photoelectric performance of GeSe₂-Sb₂Se₃-based glass ceramics by CuI doping. *Journal of Materials Science: Materials in Electronics*, 2020, 31 (2), pp.1654-1660. 10.1007/s10854-019-02683-1 . hal-02472931

HAL Id: hal-02472931

<https://univ-rennes.hal.science/hal-02472931v1>

Submitted on 11 Sep 2024

HAL is a multi-disciplinary open access archive for the deposit and dissemination of scientific research documents, whether they are published or not. The documents may come from teaching and research institutions in France or abroad, or from public or private research centers.

L'archive ouverte pluridisciplinaire **HAL**, est destinée au dépôt et à la diffusion de documents scientifiques de niveau recherche, publiés ou non, émanant des établissements d'enseignement et de recherche français ou étrangers, des laboratoires publics ou privés.

Enhanced conductivity and photoelectric performance of GeSe₂-Sb₂Se₃ based glass ceramics by CuI doping

Yang Xu^{1,3}, Hao Jin¹, Yuan Liu¹, Bo Fan², Hongli Ma³, Xianghua Zhang^{2,3}

1. College of Material and Chemistry, China Jiliang University, Hangzhou, 310018, China

2. Key Laboratory of New Lithium-ion Battery and Mesoporous Materials, College of Chemistry and Chemical Engineering, Shenzhen University, Shenzhen, 518060, China

3. Laboratory of Glasses and Ceramics, Institute of Chemical Science, University of Rennes 1, Rennes 35042, France

Abstract

CuI doped GeSe₂-Sb₂Se₃ system glass ceramics is a novel type of promising semiconductor for photoelectric application. In this study, selenide glass ceramics with different compositions were prepared by using the traditional melt-quenching method together with a 1 hour annealing process at crystallization temperature. The compositional, morphological, structural and photoelectric properties of the as-prepared glass ceramics were comprehensively investigated with XRD, SEM, TEM and photo-electrochemical system. The results show that the 20mol% CuI doped 50GeSe₂-50Sb₂Se₃ glass ceramics presents the highest conductivity which determines the migration of photo-generated charge carriers, and the highest photocurrent under visible illumination.

Keywords: Chalcogenide glass ceramics; Crystal structure; Photoelectric properties; Conductivity

Corresponding author: Yang XU (E-mail: xuyang22@cjlu.edu.cn; Tel:+86-571-87676293)

1. Introduction

As a result of the rising energy consumption and environmental crisis, researchers over the world have paid lots of attention to the development and utilization of the clean and inexhaustible solar energy [1-2]. Among a variety of solar applications, photovoltaic solar cell is considered as the most efficient way to use solar energy by directly converting solar energy into electricity [3-7]. In order to achieve high conversion efficiency, the solar cell material should have not only strong absorption in the

solar spectrum, but also efficient generation, separation and transportation of free charge carriers [8-10].

For inorganic solar cells, CdTe and CuInGaSe or their derivatives are widely studied, and each type of semiconductor always shows both advantages and disadvantages [11-15]. In the past few years, several Sb_2Se_3 based chalcogenide glasses and glass ceramics have been studied by the authors [16-18]. And, the results indicate that, while CuI is introduced into the well-known $\text{GeSe}_2\text{-Sb}_2\text{Se}_3$ system, the controlled crystallization of such chalcogenide glasses leads to transparent glass ceramics with unexpected absorption in the middle infrared region, and leads to generation of photocurrent in glass ceramics [19]. This phenomenon suggests a relatively high concentration of free charge carriers in the CuI doped chalcogenide glass ceramics. In order to promote the solar cell application of $\text{GeSe}_2\text{-Sb}_2\text{Se}_3\text{-CuI}$ glass ceramics, a comprehensive study was hence carried out in this work to investigate the photoelectric properties of the $\text{GeSe}_2\text{-Sb}_2\text{Se}_3\text{-CuI}$ glass ceramics.

2. Experimental

In this work, $\text{GeSe}_2\text{-Sb}_2\text{Se}_3\text{-CuI}$ glass ceramics with different compositions were prepared and characterized to study the effects of Ge/Sb ratio and doping dosage of CuI on the photoelectric performance of glass ceramics. The compositions studied were determined via screening the compositions prepared with the conventional melt-quenching process. The glass-forming region of the pseudo-ternary $\text{GeSe}_2\text{-Sb}_2\text{Se}_3\text{-CuI}$ system was determined as shown in Fig.1, which indicates that the doping dosage of CuI in the $\text{GeSe}_2\text{-Sb}_2\text{Se}_3$ system could be up to 30 mol%. The compositions of based glass ceramics employed include $80\text{GeSe}_2\text{-}20\text{Sb}_2\text{Se}_3$, $70\text{GeSe}_2\text{-}30\text{Sb}_2\text{Se}_3$, $60\text{GeSe}_2\text{-}40\text{Sb}_2\text{Se}_3$, $50\text{GeSe}_2\text{-}50\text{Sb}_2\text{Se}_3$ and $40\text{GeSe}_2\text{-}60\text{Sb}_2\text{Se}_3$. And, up to 30 mol% CuI was doped into each base glass composition.

The chalcogenide glasses were prepared by using the traditional melt-quenching process with a vacuum sealed silica tube vacuum. The raw materials used for glass preparation include polycrystalline germanium (99.9%), antimony (99.9%), selenium (99.9%) and CuI (98%). To prepare chalcogenide glass, required amount of each raw material were weighed according to the composition of glass and then transferred into a silica tube followed by sealing under a vacuum of around 10^{-5} mbar. The sealed tube was then transferred to a rocking furnace, which is good for the enough mixing of raw materials, and heated to 800°C at a rate of 1.5°C/min. The temperature of 800°C in furnace was kept for about 12h to ensure a complete reaction and homogenization. The furnace was then cooled down to 700°C, and the sealed tube was transferred to water for thermal quenching for 3-5s. Subsequently, the tube was annealed for 3h at a temperature close to the glass transition temperature T_g to reduce the internal stresses of glass in tube. The prepared glass rod was taken out from tube by breaking the tube and then was sliced into discs. Different glass ceramics were prepared by heating the glass discs of different compositions at corresponding crystallization onset temperatures T_x (as listed in Table 1) for 1h. All the obtained glass ceramic discs used for the following measurements have a diameter of 9mm and a thickness of 1mm.

In order to determine the glass transition temperatures T_g and the crystallization onset temperature T_x of the prepared precursor glasses for glass ceramics preparation, thermal analysis was conducted for the glasses with a differential scanning calorimeter (DSC Q20, TA Instruments). 8mg specimen of each glass sample was heated at a rate of 10°C/min for DSC analysis. The T_x of each glass sample was determined by analyzing the obtained heat flow vs temperature curves, with the results shown in table 1.

The X-ray diffraction spectra of the prepared glass ceramics were obtained with a X-ray diffraction (XRD) meter (X'PERT, PANalytical), and the scanning was conducted at a step of 0.02° within a range of 10° - 90° . Transmission electron microscope (TEM) was employed to observe the size and structure of crystals in glass ceramics, while the morphology of glass ceramics samples was observed with a scanning electron microscope (JSM-6301, JOEL). The conductivity type of glass ceramics was checked with a PN tester (PN-100, Semilab) and the electric conductivity was measured by using the four-point method. The photoelectric performance of the prepared glass ceramics were investigated by conducting the three-electrode photo-electrochemical (PEC) measurements. The three electrodes include Ag/AgCl standard electrode as the reference electrode, Pt electrode as the counter electrode, and the sample as the working electrode. The measurements were performed in an aqueous LiClO_4 (0.5 M) solution. A 150W white light tungsten halogen lamp with an intensity of 250 W/m^2 was used as the light source. And, the light from halogen lamp passed through a chopper before reaching sample surface. The current-voltage (I-V) characteristics of each glass ceramics under alternative on/off light were recorded by a potentiostat (AUTOLAB, METROHM, Herisau, Switzerland). At least 2-3 specimens were tested for each test of each sample, and the results shown were taken as the average of these test results.

3. Results and discussion

According to the DSC results, it was found that the glasses with same ratio of GeSe_2 to Sb_2Se_3 show similar crystallization behavior. As an example, Fig.2 shows the heat flow vs temperature curves of the 50GeSe_2 - $50\text{Sb}_2\text{Se}_3$ glass with different dosages of CuI. The crystallization onset temperature T_x of each glass sample were shown in Table 1. The studied GeSe_2 - Sb_2Se_3 glasses without CuI doping, regardless of the Ge/Sb ratio, were found stable against crystallization, as their characteristic temperatures at the

exothermic peak are relatively high, saying up to 350°C. However, CuI doping significantly reduces the crystallization temperature of GeSe₂-Sb₂Se₃ glass.

The main crystal phase of the ternary GeSe₂-Sb₂Se₃-CuI system is orthorhombic Sb₂Se₃, which is consistent to the cell parameters reported by Birkett [20]. Fig.3(a) shows the XRD patterns of 40GeSe₂-60Sb₂Se₃ based glass ceramics with different CuI dosage. It can be seen that CuI doping shows significant effects on the structure and hence performance of glass ceramics. When there is no CuI incorporated, the crystal phases of the GeSe₂-Sb₂Se₃ glass ceramics are mainly Se and partly Sb₂Se₃. Introducing CuI into GeSe₂-Sb₂Se₃ glass promotes the crystallization of Sb₂Se₃, leading to increase in the diffraction peak intensity of Sb₂Se₃. When the doping dosage of CuI is increased to 20 mol%, the glass system becomes unstable and a new crystalline phase Cu₂GeSe₃ with cubic phase (a = 0.555 nm) is formed [21]. However, with further increasing the CuI doping content to 30mol%, the CuI amount becomes excessive, leading to the formation of SbSeI crystal. As the energy gap of SbSeI is about 1.7 eV [22], the sunlight absorption efficiency of SbSeI is less than that of Sb₂Se₃ with an energy gap of 1.2eV. The XRD patterns of glass ceramics with different ratios of GeSe₂ to Sb₂Se₃ but same CuI doping dosage, saying 20mol%, are shown in Fig. 3(b). Sb₂Se₃ and Cu₂GeSe₃ crystals could be found in all the glass ceramics with 20mol% CuI. However, the amount of Sb₂Se₃ and Cu₂GeSe₃ crystals in different glass ceramics are different. As shown in Table 2, the characteristic peak intensity ratio of Sb₂Se₃ (221) to Cu₂GeSe₃ (111) in GeSe₂-Sb₂Se₃-CuI glass ceramics with 20mol% CuI increases from 0.32 to 2.80 with the decrease of Ge content and the increase of Sb content.

Fig.4 shows the current-voltage plots, measured with the photo-electrochemical (PEC) system, of several typical GeSe₂-Sb₂Se₃-CuI glass ceramics. It is interesting to note that intense photocurrent can be measured at both positive and negative bias, as shown in Fig.4. This indicates that the n-type and

p-type semiconducting phases simultaneously exist inside the glass ceramics [23]. Table 2 lists the photocurrent intensities of several studied glass ceramics sample. To facilitate comparison, the photocurrent intensity is taken as the difference between the light current and the dark current at the bias of -0.6V. It can be obviously observed that the photocurrent intensity of glass ceramics first increase and then decrease with the increase of the XRD peak intensity ratio of Sb_2Se_3 (221) to Cu_2GeSe_3 (111). This indicates that the Sb_2Se_3 crystal in glass ceramic is favorable for the generation of photocurrent. It is known that Sb_2Se_3 is a direct band gap semiconductor with an energy gap of 1.2 eV [24]. Previous publication [25] shows that the maximum efficiency of single junction solar cells is around 30% for materials with band gaps in the range of 1.2–1.4 eV under standard AM1.5 condition. Sb_2Se_3 could hence be considered as a suitable absorber material for photovoltaic application. When glass ceramic sample, the working electrode in PEC system, is exposed to light during PEC measurement, Sb_2Se_3 in the glass ceramics can efficiently absorb photons and promote the formation of electron-hole pairs. For the 40GeSe_2 - $60\text{Sb}_2\text{Se}_3$ glass ceramics with 20mol% CuI, its photocurrent is less than that of the 50GeSe_2 - $50\text{Sb}_2\text{Se}_3$. This is because that the excessive precipitation of Sb_2Se_3 makes the content of Cu_2GeSe_3 insufficient to form conductive channels in glass ceramics, resulting in a decrease of photocurrent.

The photocurrent is generated by the migration of photo-generated charge carriers, which is strongly related to the electrical conductivity of glass ceramics. Table 2 gives the electrical conductivities of the studied glass ceramics samples. The electrical conductivity of glass ceramics increases first and then decreases with increasing XRD peak intensity ratio of Sb_2Se_3 (221) to Cu_2GeSe_3 (111). This explains why the photocurrent increases first and then decreases with increasing

XRD peak intensity ratio of Sb_2Se_3 (221) to Cu_2GeSe_3 (111), as high conductivity is feasible for the migration of photo-generated carriers and hence the increase of photocurrent.

The conductivity of glass ceramics is dependent on the composition and structure of glass ceramics.

For example, 20mol% CuI doped $70\text{GeSe}_2\text{-}30\text{Sb}_2\text{Se}_3$ and $50\text{GeSe}_2\text{-}50\text{Sb}_2\text{Se}_3$ glass ceramics both contain Sb_2Se_3 crystal which has a conductivity of about $10^{-6} \Omega^{-1}\cdot\text{cm}^{-1}$ [26], and Cu_2GeSe_3 crystal which behaves like a metal at room temperature with a conductivity of about $5 \Omega^{-1}\cdot\text{cm}^{-1}$ [27, 28].

However, the conductivity of 20mol% CuI doped $70\text{GeSe}_2\text{-}30\text{Sb}_2\text{Se}_3$ cannot even be measured ($<10^{-8} \Omega^{-1}\cdot\text{cm}^{-1}$) and is much lower than that of the 20mol% CuI doped $50\text{GeSe}_2\text{-}50\text{Sb}_2\text{Se}_3$, although the

former glass ceramics sample contains more Cu_2GeSe_3 . Fig.5 shows the SEM images of the 20mol%

CuI doped $70\text{GeSe}_2\text{-}30\text{Sb}_2\text{Se}_3$ and $50\text{GeSe}_2\text{-}50\text{Sb}_2\text{Se}_3$ glass ceramics. It can be seen that, in the

20mol% CuI doped $70\text{GeSe}_2\text{-}30\text{Sb}_2\text{Se}_3$ glass ceramics, the Cu_2GeSe_3 crystals (determined from XRD

pattern) are fully dispersed in the glass matrix and surrounded by the amorphous phase. The insulating

amorphous glass phase amongst Cu_2GeSe_3 crystals leads to insufficient connection of Cu_2GeSe_3

crystals and hence poor conductivity of glass ceramics. As shown in Fig.5(b), when the antimony

content in glass is increased, more Sb_2Se_3 crystals with a rod-like clustered structure are formed in

20mol% CuI doped $50\text{GeSe}_2\text{-}50\text{Sb}_2\text{Se}_3$ glass ceramic, and Cu_2GeSe_3 nanocrystals would grow on the

Sb_2Se_3 crystals. This composite structure is further proved by the high resolution transmission electron

microscope (HRTEM). According to the TEM image in Fig.6(a), the obtained 20mol% CuI doped

$50\text{GeSe}_2\text{-}50\text{Sb}_2\text{Se}_3$ glass ceramic contains micrometer-sized crystalline domains. Each domain consists

of rod-like Sb_2Se_3 crystals, and interconnected nanocrystals of Cu_2GeSe_3 amongst Sb_2Se_3 crystals. This

unique structure probably provides a conductive channel in the glass ceramics, and therefore leads to

higher conductivity. Moreover, with the doping of I, the Sb_2Se_3 crystal is changed from p-type to

n-type, and the n-type Sb_2Se_3 can combine with the p-type Cu_2GeSe_3 , as shown in Fig.6(b). This promotes the formation of a p-n semiconductor nano-junction in glass ceramic, which is beneficial for the separation of photo-generated charge carriers. The nano-junction may be hence another reason for the highest photocurrent obtained in 20mol% CuI doped 50GeSe_2 - $50\text{Sb}_2\text{Se}_3$ glass ceramic. In a summary, above results indicate that the photocurrent is not only determined by the yield of photo-generated charge carriers, but also by the separation and transportation of such carriers, while the yielding, separation and transportation of charge carriers are dependent on the composition, morphology and structure of glass ceramics.

4. Conclusions

This work is devoted to a systematic study of GeSe_2 - Sb_2Se_3 -CuI system glass ceramics to maximize the photocurrent generated under visible illumination, and the effects of composition on the photoelectrical properties of glass ceramics were studied. The results show that, with decreasing Ge/Sb ratio in the composition, the amount ratio of Sb_2Se_3 to Cu_2GeSe_3 crystal in glass ceramics increases, but the conductivity and photocurrent intensity of glass ceramics increase first and then decrease. For glass ceramics with a specified Ge/Sb, CuI doping dosage affects the precipitation of crystal and the microstructure, which in turn affects the generation of photocurrent in glass ceramics. Moreover, the photocurrent generated in glass ceramics is found highly dependent on not only the composition, but also the morphology of glass ceramics. The 20mol% CuI doped 50GeSe_2 - $50\text{Sb}_2\text{Se}_3$ glass ceramics, containing micrometer-sized parallel Sb_2Se_3 rods and interconnected Cu_2GeSe_3 particles, shows a highest photocurrent. Such Sb_2Se_3 and Cu_2GeSe_3 crystals connect to each other in the glass ceramics, leading to formation of a heterojunction network. And, this unique heterojunction network structure

promotes separation of charge carriers and transportation of charge carriers by providing conductive channels, hence resulting in a high photocurrent intensity.

Aknowledgement

This work is supported by the National Natural Science Foundation of China (51802299). The authors wish to thank Qianhong Shen and Xusheng Qiao for the constructive discussion of the work.

References

1. S.A. Khalate, R.S. Kate, R.J. Deokate, A review on energy economics and the recent research and development in energy and the $\text{Cu}_2\text{ZnSnS}_4$ (CZTS) solar cells: A focus towards efficiency. *Sol. Energy* **169**, 616-633 (2018)
2. P. You, G. Tang, F. Yan, Two-dimensional materials in perovskite solar cells. *Mater. Today Energy* **11**, 128-158 (2019)
3. M.A. Green, The path to 25% silicon solar cell efficiency: History of silicon cell evolution. *Prog. Photovoltaics Res. Appl.* **17**(3), 183-189 (2010)
4. S. Sharbati, S.H. Keshmiri, Model for increased efficiency of CIGS solar cells by a stepped distribution of carrier density and Ga in the absorber layer. *Sci. China* **56**(8), 1533-1541 (2013)
5. A. Redinger, M.D. Berg, P.J. Dale, The consequences of kesterite equilibria for efficient solar cells. *J. Am. Chem. Soc.* **133**(10), 3320-3323 (2011)
6. Y. Atasoy, M.A. Olgar, E. Bacaksiz, Structural, optical and Schottky diode properties of $\text{Cu}_2\text{ZnSnS}_4$ thin films grown by two-stage method. *J. Mater. Sci. Mater. El.* **30**(11), 10435-10442 (2019)
7. M. Ramezani, A. Sobhani-Nasab, A. Davoodi, Bismuth selenide nanoparticles: simple synthesis, characterization, and its light harvesting applications in the presence of novel precursor. *J. Mater. Sci. Mater. El.* **26**(7), 5440-5445 (2015)
8. N. Liang, J. Zai, M. Xu, Q. Zhu, X. Wei, X. Qian, Novel $\text{Bi}_2\text{S}_3/\text{Bi}_2\text{O}_2\text{CO}_3$ heterojunction photocatalysts with enhanced visible light responsive activity and wastewater treatment. *J. Mater.Chem.* **2**(12), 4208-4216 (2014)
9. X. Huang, K. Wang, Y. Wang, B. Wang, L. Zhang, F. Gao, Y. Zhao, W. Feng, S. Zhang, P. Liu, Enhanced charge carrier separation to improve hydrogen production efficiency by ferroelectric

- spontaneous polarization electric field. *Appl. Catal. B-Environ.* **227**, 322-329 (2018)
10. H. Mehdizadeh-Rad, J. Singh, Combined influence of Urbach's tail width energy and mobility of charge carriers on the photovoltaic performance of bulk heterojunction organic solar cells. *J. Mater. Sci. Mater. El.* **30**(11), 10064-10072 (2019)
11. K.Q. Peng, S.T. Lee, Silicon Nanowires for Photovoltaic Solar Energy Conversion. *Adv. Mater.* **23**(2), 198-215 (2011)
12. O.K. Echendu, F.B. Dejene, I.M. Dharmadasa, An investigation of the influence of different transparent conducting oxide substrates/front contacts on the performance of CdS/CdTe thin-film solar cells. *J. Mater. Sci. Mater. El.* **28**(24), 18865-18872 (2017)
13. F. Huang, C. Yang, D. Wan, Advanced solar materials for thin-film photovoltaic cells. *Front. Phys.* **6**(2), 177-196(2011)
14. J. Wang, J. Zhu, L.L. Liao, Cu(In, Ga)Se₂ thin films prepared from stacked precursors by post-selenization process, *J. Mater. Sci. Mater. El.* **25**(4), 1863-1867 (2014)
15. J.H. Kim, S.T. Kim, L. Larina, B.T. Ahn, K. Kim, J.H. Yun, Increase in conversion efficiency of above 14% in Cu(In,Ga)₃Se₅, (β -CIGS) solar cells by Na₂S incorporation through the surface of β -CIGS film. *Sol. Energ. Mat. Sol. C* **179**, 289-296 (2018)
16. X. Zhang, Y. Xu, Q. Shen, B. Fan, X. Qiao, X. Fan, H. Yang, Q. Luo, L. Calvez, H. Ma, M. Cathelinaud, J-J. Simon, Enhancement of charge photo-generation and transport via an internal network of Sb₂Se₃/Cu₂GeSe₃ heterojunctions. *J. Mater. Chem. A* **2**(40), 17099-17106 (2014)
17. Y. Xu, B. Fan, X. Zhang, Q. Shen, M. Wang, H. Ma, Crystallization optimization of the 40GeSe₂-40Sb₂Se₃-20CuI glass for improvement of photoelectric properties. *J. Non-Cryst. Solids* **431**, 61-67 (2016)
18. Y. Xu, B. Fan, B. Xue, X. Zhang, Z. Luo, Q. Shen, H. Ma, Formation of Heterojunction Networks in the Photoelectrical Glass-Ceramics: A Thermal Analysis. *J. Am. Ceram. Soc.* **99**(8), 2639-2644 (2016)
19. Lurant Calvez, Nouveaux verres et vitrocéramiques transparents dans l'infrarouge pour l'imagerie thermique. Thesis, University of Rennes 1, 119-122 (2006)
20. M. Birkett, W.M. Linhart, J. Stoner, L.J. Phillips, K. Durose, J. Alaria, J.D. Major, R. Kudrawiec, Band gap temperature-dependence of close-space sublimation grown Sb₂Se₃ by photo-reflectance. *APL Mater.* **6**, 084901 (2018)

21. L.S. Palatnik, V.M. Koshkin, L.P. Galchinetskii, V.I. Kolesnikov, Y.F. Komnik, Mechanisms of Ordering in Ternary Semiconductors. *Fiz. Tverd. Tela.* **4**, 1430 (1962)

22. A.C. Wibowo, C.D. Mallakas, Z. Liu, J.A. Peters, M. Sebastian, D.Y. Chung, B.W. Wessels, M.G. Kanatzidis, Photoconductivity in the chalcogenide semiconductor, SbSeI: a new candidate for hard radiation detection. *Inorg. Chem.* **52**(12), 7045–7050 (2013)

23. R. Krishnan, Fundamentals of Semiconductor Electrochemistry and Photoelectro-chemistry, in: *Encyclopedia of Electrochemistry*, Wiley-VCH Verlag GmbH & Co. KGaA, (2007)

24. Y. Zhou, M. Leng, Z. Xia, J. Zhong, H. Song, X. Liu, B. Yang, J. Zhang, J. Chen, K. Zhou, J. Han, Y. Cheng, J. Tang, Solution-processed antimony selenide heterojunction solar cells. *Adv. Energy Mater.* **4**(8), 1301846 (2014)

25. C.J. Stolle, T.B. Harvey, B.A. Korgel, Nanocrystal photovoltaics: a review of recent progress, *Current Opinion in Chemical Engineering*, **2**(2), 160-167 (2013)

26. T.M. Razykov, A.X. Shukurov, O.K. Atabayev, K.M. Kuchkarov, B. Ergashev, A.A. Mavlonov, Growth and characterization of Sb₂Se₃ thin films for solar cells. *Sol. Energy* **173**, 225-228 (2018)

27. R. Wang, A. Li, T. Huang, B. Zhang, K. Peng, H. Yang, X. Lu, X. Zhou, X. Han, G. Wang, Enhanced thermoelectric performance in Cu₂GeSe₃ via (Ag,Ga)-co-doping on cation sites. *J. Alloy. Compd.* **769**, 218-225 (2018)

28. M.A. Villarreal, B.J. Fernández, M. Pirela, A. Velásquez-Velásquez, Electrical properties of the ternary compound Cu₂GeSe₃. *Rev. Mex. Fis.* **53**, 303-306 (2007)

29. C.C. Yuan, X. Jin, G.S. Jiang, W.F. Liu, C.F. Zhu, Sb₂Se₃ solar cells prepared with selenized dc-sputtered metallic precursors. *Solid State Commun. J. Mater. Sci. Mater. El.* **27**(9), 8906-8910 (2016)

30. Z. Chen, F. Chen, N.D. Tan, Controlled solvothermal synthesis of ultrahigh-aspect-ratio Sb₂Se₃ nanowires and their photoconductive properties. *Mater. Sci. Mater. El.* **26**(2), 970-977 (2015)

Figure Captions

Fig. 1. Glass forming domain of $\text{GeSe}_2\text{-Sb}_2\text{Se}_3\text{-CuI}$ system

Fig. 2. DSC curves of Series 4 glass with different CuI content

Fig. 3. XRD patterns of glass ceramics (a) in Series 5 and (b) with the fixed CuI content of 20 mol%

Fig. 4. Photoelectric properties of the typical glass ceramics measured by PEC measurement under a chopped visible light source: (a) Series 3: 20 CuI ; (b) Series 4: 20 CuI ; (c) Series 5: 20 CuI; (d) Series 5: 30 CuI

Fig. 5. SEM images of as-prepared glass ceramics: (a) Series 2: 20 CuI; (b) Series 4: 20 CuI

Fig. 6. (a)TEM image and (b) HRTEM image of the 20mol% CuI doped $50\text{GeSe}_2\text{-}50\text{Sb}_2\text{Se}_3$ glass ceramics

Figures

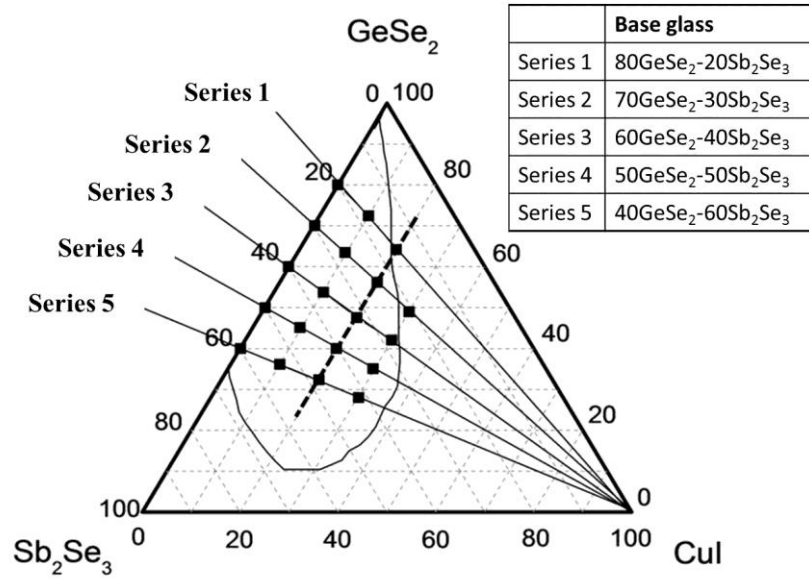


Fig. 1

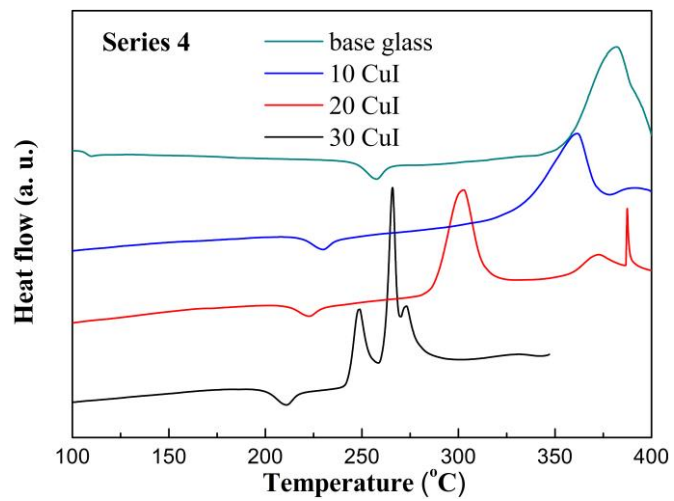


Fig. 2

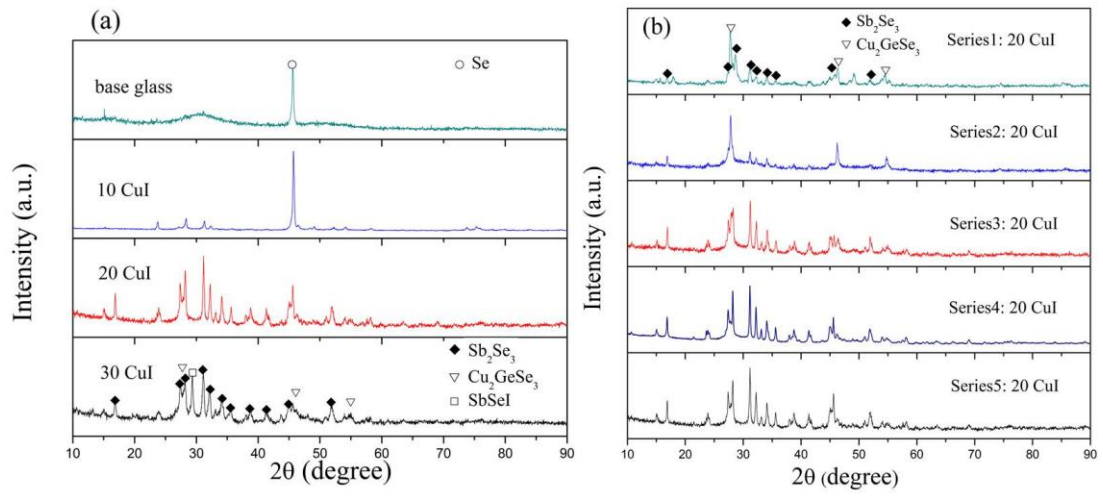


Fig. 3

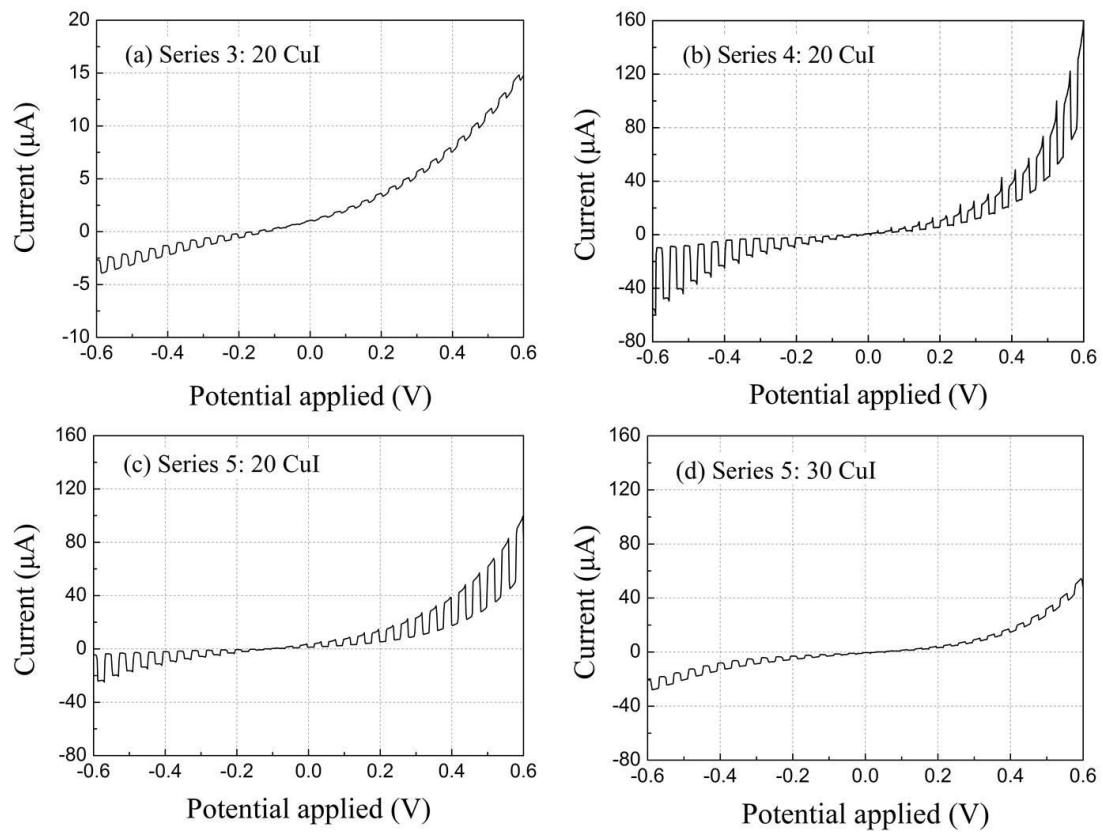


Fig. 4

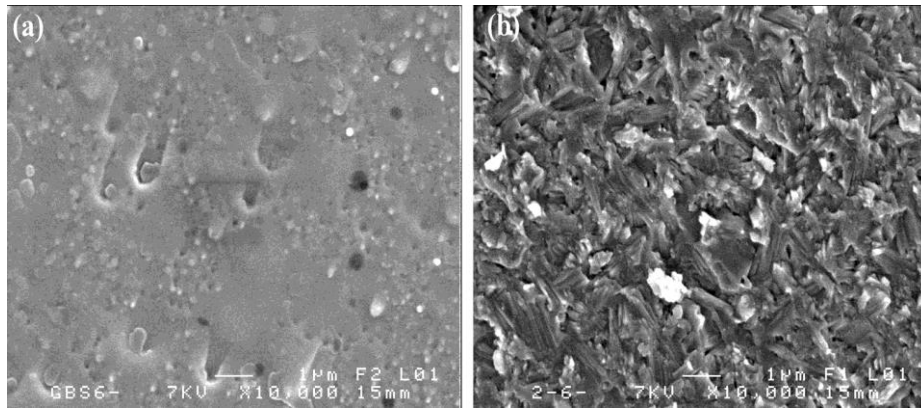


Fig. 5

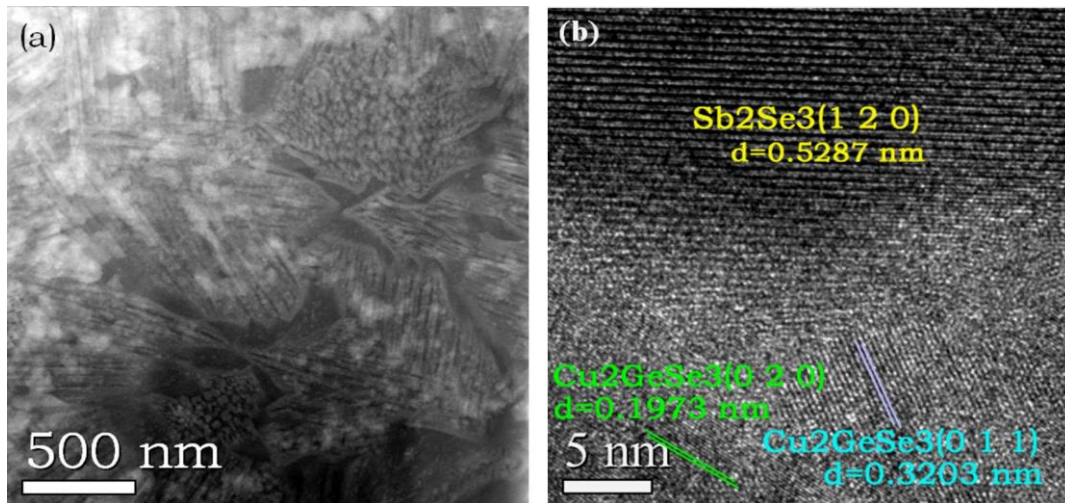


Fig. 6

Table 1 Crystallization onset temperatures of the studied GeSe₂-Sb₂Se₃-CuI system glasses

	Series 1	Series 2	Series 3	Series 4	Series 5
0 CuI	>450 °C	420 °C	404 °C	353 °C	318 °C
10 CuI	384 °C	370 °C	348 °C	324 °C	307 °C
20 CuI	369 °C	355 °C	317 °C	285 °C	287 °C
30 CuI	-	247 °C	245 °C	242 °C	250 °C

Table 2 Crystalline phase and electrical properties of some typical glass in GeSe₂-Sb₂Se₃-CuI system

	Component			XRD peak intensity ratio of Sb ₂ Se ₃ (221) to Cu ₂ GeSe ₃ (111)	Conductivity (S/cm)	Photocurrent at -0.6 V (μA/cm ²)
	GeSe ₂	Sb ₂ Se ₃	CuI			
Series 1: 20 CuI	64	16	20	0.32	<10 ⁻⁸	0
Series 2: 20 CuI	56	24	20	0.33	<10 ⁻⁸	0
Series 3: 20 CuI	48	32	20	1.29	3.3×10 ⁻⁷	2.3
Series 4: 20 CuI	40	40	20	2.68	4.4×10 ⁻²	75.0
Series 5: 20 CuI	32	48	20	2.80	3.6×10 ⁻³	33.8
Series 5: 30 CuI	28	42	30	1.44	4.7×10 ⁻³	13.2
Series 5: 10 CuI	36	54	10	-	4.5×10 ⁻⁷	0